

Lorentz-Violating Running of Coupling Constants

A.R. Vieira¹ and N. Sherrill²

¹*Universidade Federal do Triângulo Mineiro, Iturama, MG 38280-000, Brazil*

²*Department of Physics, Indiana University, Bloomington, IN 47405, USA*

We compute the full vacuum polarization tensor in the minimal QED extension. We find that its low-energy limit is dominated by the radiatively induced Chern–Simons-like term and the high-energy limit is dominated by the c -type coefficients. We investigate the implications of the high-energy limit for the QED and QCD running couplings. In particular, the QCD running offers the possibility to study Lorentz-violating effects on the parton distribution functions and observables such as the hadronic R ratio.

Spacetime anisotropy affects not only clocks and rulers but also masses and couplings. Masses and couplings appearing in the tree-level Lagrangian are just parameters, which acquire corrections due to interactions. These parameters with their quantum corrections are referred to as the physical masses and couplings. Since quantum corrections are modified in the presence of Lorentz-violating effects, it is possible to place limits on Lorentz violation by studying the running of these quantities.

In addition, the coefficient space of the QCD sector of the Standard Model Extension (SME) is comparatively unexplored.¹ Therefore, it is of interest to study how Lorentz violation affects perturbative QCD processes like $e^+e^- \rightarrow$ hadrons, deep inelastic scattering,² the Drell–Yan process, and related quantities like parton distribution functions (PDFs).⁵ In the following discussion, let us consider the modified Lagrangian of a single-flavor fermion:

$$\begin{aligned} \mathcal{L} = & \frac{1}{2} i \bar{\psi} \Gamma^\nu \overleftrightarrow{D}_\nu \psi - \bar{\psi} M \psi - \frac{1}{4} F_{\mu\nu} F^{\mu\nu} \\ & - \frac{1}{4} (k_F)_{\kappa\lambda\mu\nu} F^{\kappa\lambda} F^{\mu\nu} + \frac{1}{2} (k_{AF})^\kappa \epsilon_{\kappa\lambda\mu\nu} A^\lambda F^{\mu\nu}, \end{aligned} \quad (1)$$

where $D_\mu \equiv \partial_\mu + ieA_\mu$ is the usual covariant derivative, which couples the

gauge field with matter,

$$\Gamma^\nu = \gamma^\nu + c^{\mu\nu}\gamma_\mu + d^{\mu\nu}\gamma_5\gamma_\mu + e^\nu + if^\nu\gamma_5 + \frac{1}{2}g^{\lambda\mu\nu}\sigma_{\lambda\mu}, \quad (2)$$

and

$$M = m + m_5\gamma_5 + a_\mu\gamma^\mu + b_\mu\gamma_5\gamma^\mu + \frac{1}{2}H_{\mu\nu}\sigma^{\mu\nu}. \quad (3)$$

Considering the full fermion propagator is a difficult task. Instead, we treat the coefficients for Lorentz violation perturbatively by keeping only first-order corrections, which is appropriate given existing experimental results. There is a total of six one-loop diagrams that correct the gauge-boson propagator. Also, the regularization scheme to be applied is a subtle task. As we can see in Eq. (1), some terms contain dimension-specific objects, namely the Levi-Civita symbol and the γ_5 matrix. The inadequate choice of a regulator may cause spurious terms, especially if we are dealing with the finite part of the amplitudes. Therefore, we apply a scheme called implicit regularization.³ This scheme allows us to stay in four dimensions and does not involve spurious symmetry-breaking terms in the process of renormalization.

After computing the diagrams, we find that the low-energy limit ($p^2 \ll m^2$) of the renormalized vacuum polarization tensor is dominated by the induced Chern–Simons-like term

$$\Pi_{\text{LV}}^{\mu\nu}(p) \approx \frac{e^2}{2\pi^2}\epsilon^{\alpha\beta\mu\nu}b_\alpha p_\beta. \quad (4)$$

In computing Eq. (4), we also find contributions from the c -type and g -type coefficients from Eq. (2). However, they are suppressed relative to the dominant term by powers of p/m . Also, Eq. (4) can be affected by arbitrary and regularization-dependent surface terms. They are null if we require gauge invariance or momentum-routing invariance of the diagrams.³

By contrast, in the high-energy limit ($p^2 \gg m^2$) we find

$$\begin{aligned} \Pi_{\text{LV}}^{\mu\nu}(p) \approx & \frac{ie^2}{12\pi^2}(p^2c^{\mu\nu} - p^\mu(c^{\nu\rho} + c^{\rho\nu}) + (\mu \leftrightarrow \nu)) \left(\ln \frac{-p^2}{m^2} - \frac{5}{3} \right) + \\ & + \frac{ie^2}{6\pi^2} \left(\ln \frac{-p^2}{m^2} - \frac{13}{6} \right) c^{pp}\eta^{\mu\nu} + \frac{ie^2}{4\pi^2}c^{pp} \left(\eta^{\mu\nu} - \frac{2}{3}\frac{p^\mu p^\nu}{p^2} \right), \end{aligned} \quad (5)$$

where $c^{p\nu} \equiv c^{\mu\nu}p_\mu$. Equation (5) shows that at high energies the running couplings will effectively depend only on the c -type coefficients. It is also straightforward to show that the Ward identity is fulfilled, $p_\mu\Pi_{\text{LV}}^{\mu\nu}(p) = 0$. If we insert this finite correction into a process, like electron–muon scattering,

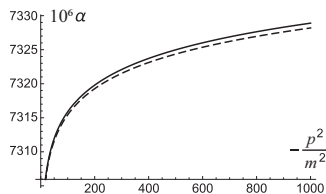


Fig. 1. Running of the QED coupling. The dashed line is the running shifted by Lorentz violation for $\frac{c^{pp}}{p^2} \sim 10^{-2}$.

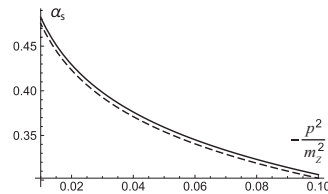


Fig. 2. Running of the QCD coupling. The dashed line is the running shifted by Lorentz violation for $\frac{c^{pp}}{p^2} \sim 10^{-1}$.

we can clearly see the c -type coefficients affect the running of the QED coupling. The amplitude of this process takes the form

$$\mathcal{M} = -\frac{1}{p^2} [\bar{u}(p_3) \Gamma_\mu(p^2) u(p_1)] e_R^2(p^2) [\bar{u}(p_4) \Gamma^\mu(p^2) u(p_2)], \quad (6)$$

where $p^2 = (p_1 - p_3)^2$ and the renormalized charge is given by $e_R^2(p^2) = e_R^2(0) \left\{ 1 + \frac{e_R^2(0)}{12\pi^2} \left[\ln \frac{-p^2}{m^2} - \frac{5}{3} - \left(\frac{2c^{pp}}{p^2} \right) \left(\ln \frac{-p^2}{m^2} - \frac{2}{3} \right) \right] \right\}$. There is also an e^2 correction in the vertex, $\Gamma_\mu(p^2) = \gamma_\mu + c_{\alpha\mu} \gamma^\alpha - \frac{e^2}{12\pi^2} c_{\alpha\mu} \gamma^\alpha \left(\ln \frac{-p^2}{m^2} - \frac{5}{3} \right)$.

We run a simulation in order to see how the couplings evolve with these corrections. This is depicted in Figs. 1 and 2 for the QED and QCD coupling, respectively. Bounds on the coefficients for Lorentz violation that come from α measurements are not so stringent; although α is very accurately known at the zero point, its measurements at higher energies have only a precision of two significant figures. However, we know the same thing happens in the running of the strong coupling α_s and QCD observables are affected by this running, so we can see how coefficients change these observables.

The result of the high-energy limit in Eq. (5) can also be used for quarks except for color and flavor factors. In the QCD computation, we also have to consider self-interacting gluon diagrams and the coefficients $k_G^{\mu\nu\alpha\beta}$ and k_{AG}^μ . The former can be taken to be traceless, i.e., $k_G^{\mu\nu\alpha}{}_\nu = 0$, because a suitable choice of coordinates can absorb this term into $c^{\mu\alpha}$. The latter decreases with the energy scale so its effects are expected to be negligible at high energies.⁴ In this way, we can focus on the c -type coefficients.

The Altarelli–Parisi equations depend on the running of α_s . Hence, a perturbative correction of the type c^{pp}/p^2 implies the PDFs depend on

Lorentz violation. It is interesting to compare this observation with recent work that shows the leading-twist unpolarized PDF may implicitly depend $c^{pp}/\Lambda_{\text{QCD}}^2$, but instead through nonperturbative effects. Quantum corrections also affect observables such as the hadronic R ratio, since it also depends on the running of α_s . Here we find

$$R = R_0 \left\{ 1 + \frac{\alpha_s(p^2)}{\pi} + \frac{\alpha_s^2(0)}{\pi} \frac{2c^{pp}}{p^2} n_f \left(\ln \frac{-p^2}{\lambda^2} - \frac{2}{3} \right) + \dots \right\}, \quad (7)$$

where R_0 is the tree-level ratio and n_f is the number of flavors.

The QCD sector of the SME also affects the tree-level ratio R_0 besides the running of α_s . There is a huge amount of data available on the R ratio from the Particle Data Group.⁶ It is possible to run a simulation in order to constrain sidereal variations of coefficients that appear using these measurements. We adapt the sidereal-time simulation of Refs. 2 for the first one hundred of these R ratio measurements. Note that this sidereal simulation is only possible if we include quantum corrections because the tree-level Lorentz-violating correction is not energy-scale dependent as the R ratio measurements are. We present the best limits in Table 1.

Table 1. Constraints on quark sidereal coefficients.

Coefficient	Constraint
$ c_q^{XY} $	$< 7.9 \times 10^{-2}$
$ c_q^{YZ} $	$< 3.4 \times 10^{-2}$
$ c_q^{XZ} $	$< 3.5 \times 10^{-2}$
$ c_q^{XX} - c_q^{YY} $	$< 1.6 \times 10^{-1}$

References

1. *Data Tables for Lorentz and CPT Violation*, V.A. Kostelecký and N. Russell, 2019 edition, arXiv:0801.0287v12.
2. V.A. Kostelecký, E. Lunghi, and A.R. Vieira, Phys. Lett. B **69**, 272 (2017); E. Lunghi and N. Sherrill, Phys. Rev. D **98**, 115018 (2018); V.A. Kostelecký and Z. Li, Phys. Rev. D **99**, 056016 (2019).
3. A.R. Vieira, A.L. Cherchiglia, and M. Sampaio, Phys. Rev. D **93**, 025029 (2016).
4. D. Colladay and P. McDonald, Phys. Rev. D **75**, 105002 (2007).
5. E. Lunghi, these proceedings; N. Sherrill, these proceedings; V.A. Kostelecký, E. Lunghi, N. Sherrill, and A.R. Vieira, arXiv:1911.04002.
6. M. Tanabashi *et al.*, Phys. Rev. D **98**, 030001 (2018).